Synthesis of Mesostructured Lamellar Aluminophosphates Using Supramolecular Templates†

Abdelhamid Sayari,* Igor Moudrakovski, and Jale Sudhakar Reddy

Department of Chemical Engineering, Université Laval, Ste-Foy, Qc, Canada G1K 7P4

Christopher I. Ratcliffe, John A. Ripmeester, and Keith F. Preston

Steacie Institute for Molecular Sciences, National Research Council, Ottawa, Ont, Canada K1A 0R6

Received January 17, 1996. Revised Manuscript Received April 8, 1996⊗

The liquid-crystal templating approach for the synthesis of mesostructured materials was extended to aluminophosphates. A variety of lamellar $AlPO_4$ phases with *d* spacings in the nanometer range were prepared in the presence of long-chain primary and tertiary amines. A systematic study of the influence of the gel composition was carried out. $AlPO_4$ materials were characterized by various techniques including XRD, TEM, electron diffraction, and ^{27}Al, ^{31}P, ^{15}N, and ^{13}C NMR. The gel composition has a drastic influence on the nature of the product formed and on the coordination of aluminum and phosphorus in the final "crystalline" phase. These lamellar $AlPO_4$ phases were not stable under calcination conditions and the templating surfactant could not be removed by solvent extraction.

Introduction

Since their discovery by Mobil's researchers,[1] the crystalline mesoporous molecular sieves, designated M41S, have attracted many scientists. These materials, which crystallize mainly in layered, hexagonal, or cubic structures were prepared hydrothermally using mostly long-chain alkyltrimethylammonium salts as templates. Other types of ionic and neutral surfactant templates were also used.[2,3] The hexagonal MCM-41 phase with its uniform pore system with adjustable sizes from 16 to 100 Å seems to offer the most promising properties for potential applications in catalysis and in the area of advanced materials.[4] The synthesis and catalytic applications of these materials were reviewed recently.[5] The main steps in the synthesis of crystalline mesoporous silicates involve the formation of surfactant−silicate ion pairs, their organization into a mesophase, and the condensation of the silicate species to give inorganic layers or walls.[1,3,6,7] There is ample evidence that the silicate ions generated in the reaction medium influence the ordering of the surfactant molecules leading to the formation of one of the three mesophases: hexagonal, cubic, or lamellar, depending on the pH, the concentration of surfactant and other ingredients and the temperature.[1,3,6,7]

Earlier investigations focused mainly on mesoporous silicates and aluminosilicates.[1,8] Further work dealt with two main issues: (i) the modification of silica mesoporous materials by small amounts of metal cations such as Ti,[9] V,[10] and B;[11] (ii) the synthesis of other oxide-based mesoporous materials.[12] Huo et al.[12] reported on

† Published as NRCC No. 39104.

* To whom all correspondence should be addressed. Email: sayari@gch.ulaval.ca.

⊗ Abstract published in *Advance ACS Abstracts,* July 15, 1996.

(1) (a) Kresge, C. T.; Leonowicz, M. E.; Vartuli, J. C.; Beck, J. S. *Nature* **1992**, *359*, 710. (b) Beck, J. S.; Vartuli, J. C.; Roth, W. J., Leonowicz, M. E.; Kresge, C. T.; Schmitt, K. D.; Chu, C. T. W.; Olson, D. H.; Sheppard, E. W.; McCullen, S. B.; Higgins, J. B.; Schlenker, J. L. *J. Am. Chem. Soc.* **1992**, *114*, 10834.

(2) (a) Tanev, P. T.; Pinnavaia, T. J. *Science* **1995**, *267*, 865. (b) Bagshaw, S. A.; Prouzet, E.; Pinnavaia, T. J. *Science* **1995**, *269*, 1242.

(3) Huo, Q.; Margolese, D. I.; Ciesla, U.; Feng, P.; Gier, T. E.; Sieger, P.; Leon, R.; Petroff, P. M.; Schüth, F; Stucky, G. D. *Nature* **1994**, *368*, 317.

(4) (a) Pelrine, B. P.; Schmitt, K. D.; Vartuli, J. C. U.S. Patent 5,-105,051, 1992. (b) Beck, J. S.; Socha, R. F.; Shihabi, D. S.; Vartuli, J. C. U.S. Patent 5,143,707, 1992. (c) Le, Q. N.; Thompson, R. T.; Yokomizo, G. H. U.S. Patent 5,134,242, 1992. (d) Le, Q. N.; Thompson, R. T. U.S. Patent 5,232,580, 1993. (e) Le, Q. N. U.S. Patent 5,118,894, 1992. (f) Kloetstra, K. R.; van Bekkum, H. *J. Chem. Soc., Chem. Commun.* **1995**, 1005. (g) Corma, A.; Martinez, A.; Martinez-Soria, V.; Monton, J. B. *J. Catal.* **1995**, *153*, 25. (h) Roos, K.; Liepold, A.; Reschetilowski, W.; Schmidt, R.; Karlsson, A.; Stocker, M. *Stud. Surf. Sci. Catal.* **1995**, *94*, 389. (i) Wu, C. G.; Bein, T. *Science* **1994**, *264*, 1757. (j) Wu, C. G.; Bein, T. *Chem Mater.* **1994**, *6*, 1109. (k) Wu, G. C.; Bein, T. *Science* **1994**, *266*, 1013. (l) Corma, A.; Fornés, V.; Garcia, H.; Miranda, M. A.; Sabater, M. J. *J. Am. Chem. Soc.* **1994**, *116*, 9767. (m) Beck, J. S.; Kuel, G. H.; Olson, D. H.; Schlenker, J. L.; Stucky, G. D.; Vartuli, J. C. U.S. Patent 5,348,687, 1994. (n) Olson, D. H.; Stucky, G. D.; Vartuli, J. C. U.S. Patent 5,364,797, 1994.

(5) (a) Sayari, A. *Chem. Mater.*, in press. (b) Sayari, A. In *Recent Advances and New Horizons in Zeolite Science and Technology*; Chon, H., et al., Eds., Elsevier: Amsterdam, in press.

(6) Monnier, A.; Schüth, F.; Huo, Q.; Kumar, D.; Margolese, D.; Maxwell, R. S.; Stucky, G. D.; Krishnamurthy, M.; Petroff, P.; Firouzi, A.; Janicke, M; Chmelka, B. F. *Science* **1993**, *261*, 1299.

(7) Vartuli, J. C.; Schmitt, K. D.; Kresge, C. T.; Roth, W. J.; Leonowicz, M. E.; McCullen, S. B.; Hellring, S. D.; Beck, J. S.; Schlenker, J. L.; Olson D. H.; Sheppard, E. W. *Chem. Mater.* **1994**, *6*, 2317.

(8) (a) Chen, C. Y.; Li, H. X.; Davis, M. E. *Microporous Mater.* **1993**, *2*, 17. (b) Chen, C. Y.; Burkett, S. L.; Li, H. X.; Davis, M. E. *Microporous Mater.* **1993**, *2*, 27. (c) Corma, A.; Fornes, V.; Navarro, M. T.; Perez-Pariente, J. *J. Catal.* **1994**, *148*, 569.

(9) (a) Tanev, P. T.; Chibwe, M.; Pinnavaia, T. J. *Nature* **1994**, *368*, 321. (b) Corma, A.; Navarro, M. T.; Perez-Pariente, J. *J. Chem. Soc., Chem. Commun.* **1994**, 147. (c) Sayari, A.; Karra V. R.; Reddy, J. S. *Mater. Res. Soc. Symp. Proc.* **1995**, *371*, 87. (d) Sayari, A.; Reddy, K. M.; Moudrakovski, I. L. *Stud. Surf. Sci. Catal.* **1995**, *98*, 19.

(10) (a) Reddy, K. M.; Moudrakovski, I. L.; Sayari, A. *J. Chem. Soc., Chem. Commun.* **1994**, 1059. (b) Sayari, A.; Moudrakovski, I. L.; Ratcliffe, C.; Ripmeester, J.; Preston, K. F. In *Synthesis of Microporous Materials: Zeolites, Clays and Nanostructures*; Kessler, H., Occelli, M., Eds.; Marcel Dekker: New York, in press. (c) Reddy, J. S.; Sayari, A. *J. Chem. Soc., Chem. Commun.* **1995**, 2231. (d) Reddy, J. S.; Sayari, A. *Appl. Catal.*, submitted for publication.

(11) (a) Sayari, A.; Danumah, C.; Moudrakovski, I. L. *Chem. Mater.* **1995**, *7*, 813. (b) Sayari, A.; Moudrakovski, I. L.; Danumah, C.; Ripmeester, J.; Ratcliffe, C.; Preston, K. F. *J. Phys. Chem.* **1995**, *99*, 16373.

S0897-4756(96)00029-4 CCC: $12.00

open-structure networks of various metal oxides such as W, Sb, Zn, Pb, Mg, Al, Mn, Fe, Co, Ni, and Zn oxides. These materials were prepared in the presence of both anionic (sulfate, phosphate, and carboxylate) and cationic (quaternary ammonium salts) surfactants. In most cases, the final phase was lamellar, except for W (hexagonal and lamellar), Sb (hexagonal and cubic), and Pb (hexagonal and lamellar) oxides. However, all the layered phases and even hexagonal phases of W, Sb, and Pb oxides collapsed upon calcination. More recently, hexagonally packed mesoporous titania with relatively high stability was synthesized.[13] Abe et al.[14] prepared hexagonal vanadium−phosphorus oxides using alkyltrimethylammonium chloride. We also succeeded in preparing both lamellar and hexagonal ZrO_2 using the same supramolecular templating technique.[15]

Aluminophosphates ($AlPO_4$) are a class of microporous materials with close structural and chemical similarities with aluminosilicate zeolites.[16] Some ultralarge-pore members of this family have been synthesized.[17] These include VPI-5[18] and JDF-20[19] which have 18- and 20-membered ring openings, respectively. Cloverite is an ultralarge-pore gallophosphate molecular sieve with 20-membered ring channels.[20] Aluminophosphates are usually prepared hydrothermally in the presence of amine templates.[21] The use of linear alkylenediamines[22] or cyclic diamines[23] afforded lamellar aluminophosphates.

Recently, we extended for the first time the so-called liquid-crystal templating mechanism to the synthesis of lamellar aluminophosphates with d-spacings in the nanometer range.[24,25a] This paper is a detailed report on such materials.

Experimental Section

The $AlPO_4$ materials described here will be referred to as $AlPO_4$ *x*:*y*:*z*:*w*. They were prepared using the following molar gel composition:

$$x\mathrm{P_2O_5}{:}y\mathrm{Al_2O_3}{:}z\text{R-NR}'_2{:}w\mathrm{H_2O}$$

where $x = 1.0$ (or 0 for some P free samples), $y = 0-2.0$, $z = 0.125-2.0$, and $w = 60-300$. Notice that w corresponds to the amount of water added, i.e., it does not include water contained in the starting materials catapal B alumina and H_3PO_4 solution. The template $R-NR'_2$ was a primary ($R' = H$) or a tertiary ($R' = CH_3$) amine with a long alkyl chain ($R = C_nH_{2n+1}$).

In a typical synthesis, 2.42 g of alumina (72% pseudoboehmite alumina, catapal B from Vista) in 5 g of water was reacted with 4 g of phosphoric acid (Fisher Scientific, 85%) diluted with 13 g of water and stirred for about 1 h. Finally 3.2 g of dodecylamine surfactant was added to this mixture, and stirred for an additional hour. This batch corresponds to the following molar gel composition: $P_2O_5{:}Al_2O_3{:}C_{12}H_{25}NH_2{:}60\ H_2O$. The final reaction mixture was transferred into a 150 cm^3 Teflon-lined autoclave. Unless otherwise stated, the crystallization was carried out at 373 K for 24 h without any agitation. Subsequently, the autoclave was quenched in cold water and the product was filtered, washed with deionized water, and dried at ambient temperature.

X-ray diffraction (XRD) measurements were made on a D5000 Siemens diffractometer, using Cu Kα radiation (λ = 0.154 18 nm). Transmission electron micrographs were obtained as reported elsewhere.[25] ^{31}P and ^{27}Al magic angle spinning (MAS) NMR spectra were obtained on a Bruker AMX-300 instrument (Magnetic field 7.05 T, Larmor frequencies 78.18 and 121.47 MHz, respectively). Typical MAS speeds of rotation were 10−14 kHz, and the delay times were set at 60 s for ^{31}P and 0.3 s for ^{27}Al. A conventional one-pulse sequence in combination with high-power proton decoupling (40 kHz) was used for both nuclei. Very short radiofrequency pulses were employed for ^{27}Al (0.6 μs, π/18 for liquids) in order to obtain spectra for quantitative measurements.[26] All ^{27}Al MAS and some ^{31}P MAS spectra were also recorded at 14.1 T on a Bruker AMX 600 spectrometer (Larmor frequencies 156.36 and 242.95 MHz). Some ^{27}Al MAS NMR spectra were also obtained at 4.7 T (frequency 52.11 MHz) on a Bruker MSL 200 spectrometer. A 5 mm high-speed probe and a 5 mm Ultrasonic Speed Probe, both from DOTY Scientific, were used on the AMX 300/MSL 200 and AMX 600, respectively. 85% H_3PO_4 and a 1 M solution of aluminum nitrate were used as external references. All values for the ^{27}Al chemical shifts reported in the text and tables were corrected for the second order quadrupolar interactions.[27] Simulations and deconvolutions of the spectra were performed with the WinFit software package from Bruker.

^{13}C and ^{15}N NMR spectra were collected with cross-polarization and magic angle spinning (CP MAS) on a Bruker AMX-300 spectrometer (Larmor frequencies 75.5 and 30.1 MHz, respectively). In both cases a 5 mm high-speed probe from DOTY Scientific was used. The speed of rotation was within 3−3.5 kHz, and the CP contact time was 2 and 5 ms for ^{13}C and ^{15}N, respectively. Signals from tetramethylsilane (TMS) and the NO_3^- group of solid NH_4NO_3 were used as external references.

Results and Discussion

Unlike M41S and other mesostructured transition-metal oxides, which are usually prepared in the presence of ionic surfactants, the templates we used were either long-chain primary alkylamines or tertiary dimethylalkylamines. Earlier, long-chain alkylamines were used as templates for the preparation of pure and transition-metal-modified hexagonal mesoporous silicates (HMS).[2a,9ac,10,28]

The gel composition and chemical analysis of some of the $AlPO_4$ samples we prepared are reported in Table

(12) Huo, Q.; Ciesla, D. I.; Demuth, D. G.; Feng, P.; Gier, T. E.; Sieger, P.; Firouzi, A.; Chmelka, B. F.; Schüth, F.; Stucky, G. D. *Chem. Mater.* **1994**, *6*, 1176.
(13) Antonelli, D. M.; Ying, J. Y. *Angew. Chem., Int. Ed. Engl.* **1995**, *34*, 2014.
(14) Abe, T.; Taguchi, A.; Iwamoto, M. *Chem. Mater.* **1995**, *7*, 1429.
(15) Reddy, J. S.; Sayari, A. *Catal. Lett.*, in press.
(16) Wilson, S. T.; Lok, B. M.; Messina, C. A.; Connan, T. R.; Flanigen, E. M. *J. Am. Chem. Soc.* **1982**, *104*, 1146.
(17) Davis, M. E., Ed. *Catal. Today* **1994**, *19*.
(18) Davis, M. E.; Montes, C.; Garces, J. M. *ACS Symp. Ser.* **1989**, *398*, 291.
(19) Huo, Q.; Xu, R.; Li, S.; Ma, Z.; Thomas, J. M.; Jones, R. H.; Chippindale, A. M. *J. Chem. Soc., Chem. Commun.* **1992**, 875.
(20) Estermann, M.; McCusker, L. B.; Baerlocher, C.; Merrouche, A.; Kessler, H. *Nature* **1991**, *352*, 320.
(21) Wilson, S. T. *Stud. Surf. Sci. Catal.* **1991**, *58*, 137.
(22) (a) Jones, R. H.; Thomas, J. M.; Xu, R.; Huo, Q.; Cheetham, A. K.; Powell, A. V. *J. Chem. Soc., Chem. Commun.* **1991**, 1266. (b) Thomas, J. M.; Jones, R. H.; Xu, R.; Chen, J.; Chippindale, A. M.; Natarajan, S.; Cheetham, A. K. *J. Chem. Soc., Chem. Commun.* **1992**, 929. (c) Jones, R. H.; Chippindale, A. M.; Natarajan, S.; Thomas, J. M. *J. Chem. Soc., Chem. Commun.* **1994**, 565. (d) Kraushaar-Czarnetzki, B.; Stork, W. H. J.; Dogterom, R. J. *Inorg. Chem.* **1993**, *32*, 5029.
(23) Barrett, P. A.; Jones, R. H. *J. Chem. Soc., Chem. Commun.* **1995**, 1979.
(24) Sayari, A.; Karra, V. R.; Reddy, J. S.; Moudrakovski, I. L. *J. Chem. Soc., Chem. Commun.* **1996**, 411.
(25) (a) Chenite, A.; Le Page, Y.; Karra, V. R.; Sayari, A. *J. Chem. Soc., Chem. Commun.* **1996**, 413. (b) Chenite, A.; Le Page, Y.; Sayari, A. *Chem. Mater.* **1995**, *7*, 1015.
(26) Mann, P. P.; Klinowski, J.; Trokiner, A.; Zanni, H.; Papon, P. *Chem. Phys. Lett.* **1988**, *151*, 143.
(27) Engelhardt, G.; Michel, D. *High-Resolution Solid-State NMR of Silicates and Zeolites*, Wiley: Chichester, 1987.
(28) (a) Reddy, J. S.; Dicko, A.; Sayari, A. In *Synthesis of Microporous Materials: Zeolites, Clays and Nanostructures*; Kessler, H., Occelli, M., Eds., Marcel Dekker: New York, in press.

Table 1. Synthesis Parameters, *d* Spacings and Chemical Analysis of $AlPO_4$ Samples Prepared Using Primary Alkylamines

sample no.	template	input[a] *x*:*y*:*z*	*d* spacing,[b] (Å) 1	2	analysis[c] P:Al	analysis[d] P:Al
1	$C_{12}-NH_2$	1:0.2:1	22.6			
2	$C_{12}-NH_2$	1:0.4:1	22.6		1:0.54	
3	$C_{12}-NH_2$	1:0.6:1	29.7			
4	$C_{12}-NH_2$	1:0.8:1	32.5		1:0.92	1:0.80
5	$C_{12}-NH_2$	1:1.0:1	32.5		1:1.05	1:0.79
6	$C_{12}-NH_2$	1:1.2:1	33.2		1:1.26	1:0.84
7	$C_{12}-NH_2$	1:1.4:1	32.7		1:1.47	1:0.90
8	$C_{12}-NH_2$	1:1.6:1	32.2		1:1.69	1:0.95
9	$C_{12}-NH_2$	1:1.8:1	32.2		1:1.84	1:0.89
10	$C_{12}-NH_2$	1:2.0:1	32.7		1:2.11	1:1.07
11	$C_{12}-NH_2$	1:1:0.125	amorphous			
12	$C_{12}-NH_2$	1:1:0.25	amorphous			
13	$C_{12}-NH_2$	1:1:0.5	36.5	(32.7)	1:1.02	
14	$C_{12}-NH_2$	1:1:0.75	34.0		1:1.05	
5	$C_{12}-NH_2$	1:1:1.0	32.5		1:1.05	
15	$C_{12}-NH_2$	1:1:1.5	(30.7)	37.1	1:1.04	
16	$C_{12}-NH_2$	1:1:2.0	(30.3)	37.7	1:1.05	
17	C_8-NH_2	1:1:1	28.0		1:1.18	
18	$C_{10}-NH_2$	1:1:1	30.1		1:1.11	
5	$C_{12}-NH_2$	1:1:1	32.5		1:1.05	
19	$C_{10}-NH_2$	1:0:1	20.4			
20	$C_{12}-NH_2$	1:0:1	22.3			
21	$C_{12}-NH_2$	0:1:1	amorphous			

[a] All samples had $w = 60$. [b] The *d* distances given in parentheses correspond to a minor phase. [c] Bulk composition. [d] Framework composition.

1. The overall Al and P ratios in the as-synthesized products were comparable to the corresponding ratios in the synthesis gels. The pH of the gels was quite low; and varied during the gel preparation from ca. 2.5 to 3.5. As a result, the template occluded in the as-synthesized sample was protonated. This conclusion directly follows from ^{15}N and ^{13}C NMR data of the materials. The ^{15}N isotropic chemical shift for pure solid dodecylamine is −346.0 ppm, while for the 1:1 dodecylamine−phosphoric acid complex (sample no. 20) the shift is −339.6 ppm. For dodecylamine occluded in $AlPO_4$ samples with the same template to phosphorus ratio the shift is always within -340.0 ± 0.4 ppm. The ^{13}C chemical shift for the C_1 carbon of the dodecyl group was 43.1 ppm for pure dodecylamine and 40.6 ppm for dodecylamine−phosphoric acid complex (sample No. 20). The ^{13}C chemical shift for the dodecylamine occluded in $AlPO_4$ samples was 40.2 ± 0.4 ppm, thus additionally indicating that protonation has occurred. The observed ^{15}N and ^{13}C chemical shifts for the pure amine and its protonated forms are well within the regions expected from available liquid-state ^{13}C and ^{15}N NMR data.[29,30]

XRD patterns of a series of $AlPO_4$ samples prepared from the gels with different Al_2O_3/P_2O_5 ratios are shown in Figure 1. The occurrence of lamellar phases was inferred from the presence of only diffraction peaks that are higher orders of the first (001) peak. The transmission electron micrograph of $AlPO_4$ 1:1:1:60 (sample no. 5, Table 1) shown in Figure 2 also clearly indicates the occurrence of lamellar $AlPO_4$ structures. Additional TEM data may be found elsewhere.[24,25a]

Calcination of the lamellar $AlPO_4$ material at 773 K (heating rate 1 K min^{-1}) in a quartz cell under a flow

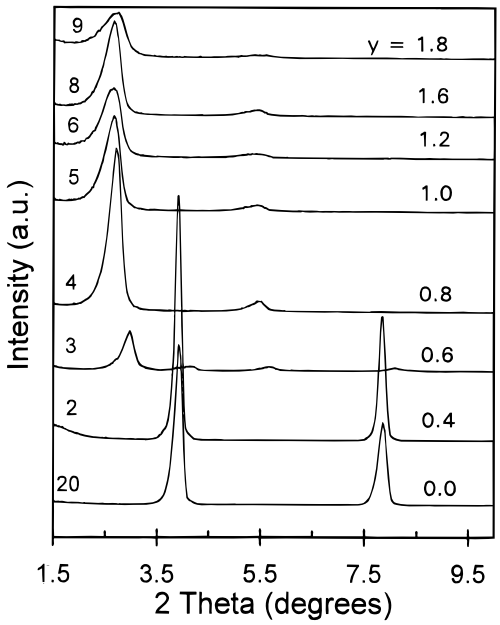

Figure 1. XRD patterns of various as-synthesized $AlPO_4$ 1:*y*:60 samples prepared with variable amounts of alumina. Numbers on the right-hand side indicate the sample number given in Table 1.

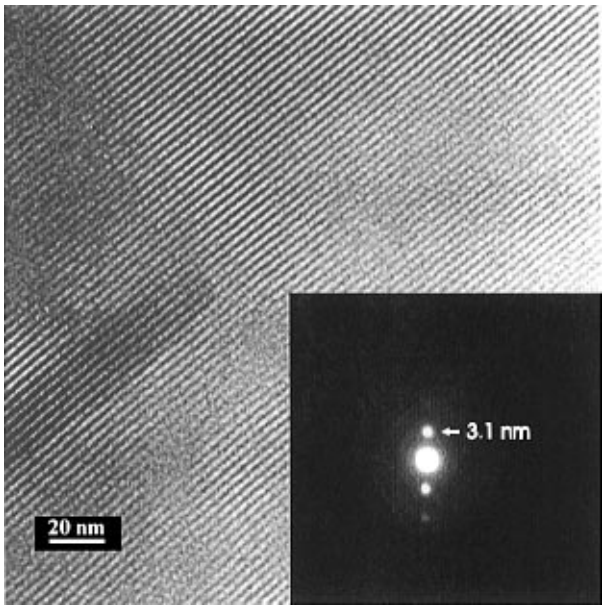

Figure 2. TEM micrograph of $AlPO_4$ 1:1:1:60 (sample no. 5), from ref 25a.

of nitrogen followed by air resulted in the collapse of the lamellar structure. Numerous attempts were made to prepare such $AlPO_4$ materials with three-dimensional rather than lamellar structure by modifying the composition of the starting synthesis mixture. Our systematic approach consisted of changing the amount relative to P_2O_5 of all other starting materials one at a time. In addition to the effect of Al_2O_3/P_2O_5, $R-NR'_2/P_2O_5$, and H_2O/P_2O_5 ratios, the effects of alkylamine chain length, crystallization temperature, and time were studied. In the following sections, we discuss the influence of these factors on the products. Unless otherwise mentioned, the syntheses were carried out using primary amines, mainly dodecylamine, as templates.

Influence of Al_2O_3 / P_2O_5 Ratio. As seen in the upper part of Table 1 (sample nos. 1−10), the amount of Al was varied gradually while keeping the number

(29) Witanowski, M.; Stefaniak, L.; Webb, G. *Nitrogen NMR Spectroscopy Annual Reports on NMR Spectroscopy*; Academic Press: London, 1982; Vol. 14.

(30) Breitmaier, E.; Voelter, W. *^{13}C NMR Spectroscopy*; Verlag-Chemie: New York, 1978.

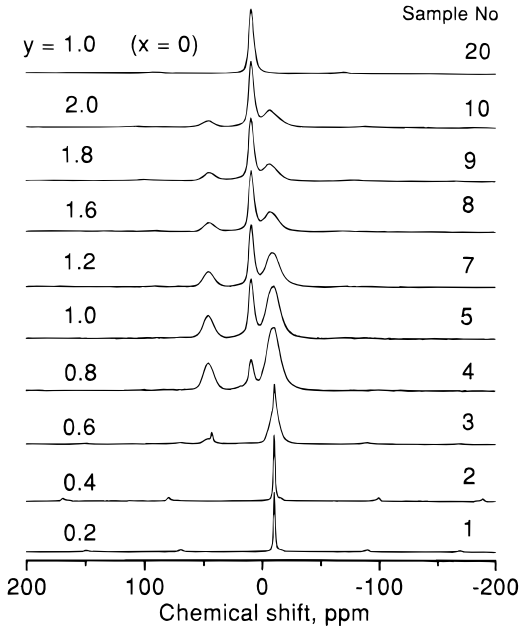

Figure 3. ^{27}Al MAS NMR spectra of $AlPO_4$ 1:*y*:1:60 samples prepared with variable amounts of alumina.

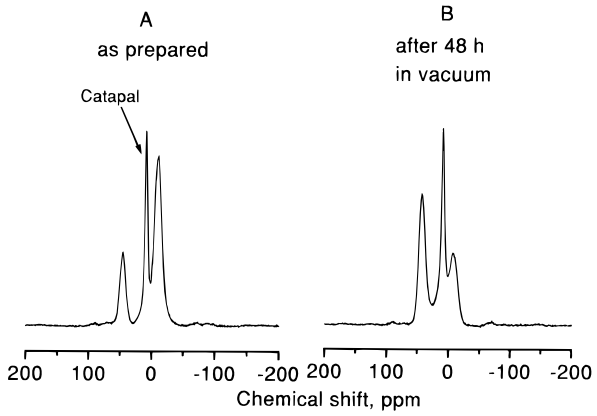

Figure 4. ^{27}Al MAS NMR spectra (H_0 = 14.1 T) of as-synthesized (A) and dehydrated (B) $AlPO_4$ 1:1:1:60 sample (sample no. 5).

of moles of phosphorus, surfactant, and added water constant ($x = z = 1$, $w = 60$). These variations in the gel composition did not lead to other structures than lamellar $AlPO_4$s. It is interesting to note that even in the absence of aluminum, a lamellar surfactant−phosphoric acid complex was obtained (sample no. 20). However, when aluminum was used without phosphorus, only amorphous materials were achieved (sample no. 21).

Figures 3−5 show the ^{27}Al and ^{31}P NMR spectra of $AlPO_4$ samples with different Al/P ratios. Data concerning the spectra are summarized in Table 2. Figure 3 reports the ^{27}Al MAS NMR spectra of samples with increasing aluminum content (sample nos. 20 and 1−10) prepared using the following gel composition: P_2O_5:yAl_2O_3:C_{12}−NH_2:60 H_2O with $y = 0$−2. In general, three signals with different chemical shifts were observed. The signal at 47.0 ± 0.7 ppm was assigned to tetrahedral aluminum bonded to phosphorus atoms via oxygen bridges. In the literature, for various microporous $AlPO_4$ materials, signals in the range 35−48 ppm (usually not corrected for the second-order quadrupolar interaction, which shifts the signals to high field from the real position) were reported as characteristic of tetrahedral aluminum surrounded by four PO_4 groups.[31] We attributed the peak in the range −6 to −10 ppm to the framework octahedral aluminum coordinated with water and PO_4 groups.[32−35] Previously, it was shown that the chemical shift of six-coordinated aluminum changes almost linearly with the number of

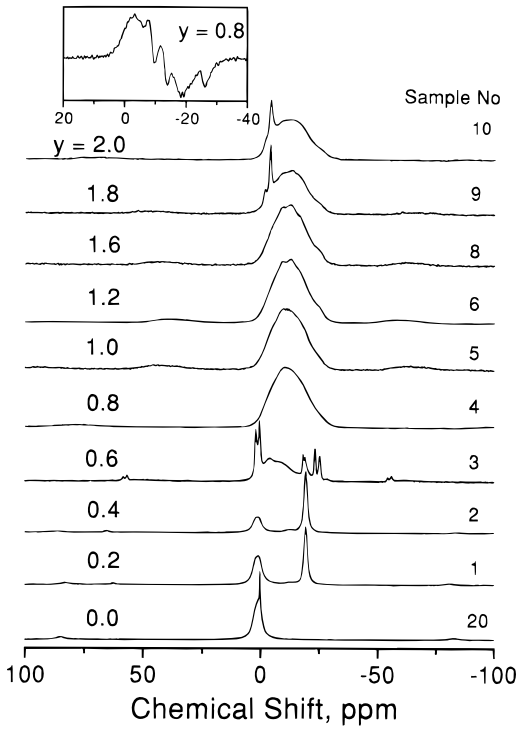

Figure 5. ^{31}P MAS NMR spectra of $AlPO_4$ 1:*y*:1:60 samples prepared with variable amounts of alumina. Spectra of samples with y = 0.6, 1.0, 1.2, 1.6, and 1.8 were recorded at high frequency (14.1 T). Inset: first derivative of the ^{31}P spectra of $AlPO_4$ 1:1.2:1:60 (sample no. 6).

Table 2. ^{31}P and ^{27}Al NMR of $AlPO_4$ Samples Prepared Using Primary Alkylamines as Surfactants[a]

sample no.[b]	^{31}P (ppm)	^{27}Al (T_d) (ppm)	^{27}Al (O_h) (ppm)	^{27}Al (O_h) (ppm)
20	0.6; 2.3 s			
1	1.0 s; −19.3 s			−9.8 sh
2	1.0 s; −19.0 s			−9.9 sh
3	0.65 s; 2.26 s; −18.6 s	47.4 sm		−10.2 s
	−19.1 s; −23.8 s; −25.8 s	44.5 sm		
4	−13.0 b	47.7 m,b	10.4 m,sh	−8.5 s,b
5	−13.0 b	46.8 m,b	10.4 s,sh	−8.7 s,b
6	−13.0 b	46.5 m,b	10.5 s,sh	−8.5 m,b
7	−13.0 b	47.5 sm,b	10.4 s,sh	−8.0 sm,b
8	−13.0 b	46.8 sm,b	10.7 s,sh	−6.8 sm,b
9	−3.8 s; −13.0 b	46.8 sm,b	10.4 s,sh	−6.6 sm,b
10	−3.0 s; −13.0 b	46.3 sm,b	10.0 s,sh	−6.5 sm,b
21			10.3 s,sh	
13	−1.0 s; −19.0 s	46.8 sm		−10.1 s,sh
14	−13.0 b; −19.1 s	47.0 sm,b	10.4 s,sh	−7.8 s,sh
5	−13.0 b	46.8 m,b	10.4 s,sh	−8.7 s,b
15	−1.4; −3.7 s; −20.0 sm	45.0 sm	10.1 sm	3.0 q
16	−1.5; −3.6 s			3.0 q
17	0.3; 1.6	46.8 sm,b	10.1 s	−8.9 b
18	−13.0 b	46.6 sm,b	10.3 s	−9.3 b

[a] b, broad; q, line shape dominated by the quadrupolar interaction; m, medium; s, strong; sh, sharp: sm, small. [b] Sample compositions were given in Table 1.

(31) Muller, D.; Jahn, E.; Ladwig, G.; Haubenreisser, V. *Chem. Phys. Lett.* **1984**, *109*, 332.
(32) Zubowa, H. L.; Alsdorf, E.; Fricke, R.; Neissendorfer, F.; Richter-Medau, J.; Schreier, E.; Zeigan, D.; Zibrowins, B. *J. Chem. Soc., Faraday Trans.* **1990**, *86*, 2307.
(33) Goepper, M.; Guth, F.; Delmotte, L.; Guth, J. L.; Kessler, H. *Stud. Surf. Sci. Catal.* **1989**, *49B*, 857.
(34) Hasha, D.; Saldarriaga, L.; Saldarriaga, C.; Hathaway, P. E.; Cox, D. F.; Davis, M. E. *J. Am. Chem. Soc.* **1988**, *110*, 2127.
(35) Blackwell, C. S.; Patton, R. L. *J. Phys. Chem.* **1988**, *92*, 3965.

phosphate groups in its coordinated shell, starting from 0 for $Al(H_2O)_6^{3+}$ and reaching −18 ppm for aluminum metaphosphate, where aluminum is coordinated to six PO_4 groups.[36] Our present assignment is also supported by the data of Rocha et al.,[37] who for $Al(OP)_4(OH_2)_2$ sites observed signals between −9.5 and −12 ppm.

The presence of water in the coordination shell of aluminum is further evidenced by the fact that treatment of the samples under vacuum brought about a significant decrease in the intensity of the peak at −10 ppm in favor of the peak at 47 ppm (Figure 4). This result indicates that both species are related to each other and that at least two ligands of the octahedral aluminum species are water molecules.

An additional signal in the ^{27}Al spectra, which was observed only for Al/P ratios higher than 0.8, has a chemical shift of 10.3 ± 0.4 ppm. Since the amorphous P-free sample (sample no. 21) gives only one ^{27}Al NMR peak at the same position, we assign the signal to the unreacted Al source, pseudoboehmite (catapal B). Employment of high spinning speed, extrahigh magnetic field, and short radiofrequency pulses allowed accurate determination of the relative concentrations of this extraframework aluminum. Combination of this relative integral intensity information with bulk Al/P ratio obtained by chemical analysis gives us the Al/P ratio in the lattice of the materials. It was assumed that all phosphorus used remains in the final product. The resulting Al/P ratios are given in the last column of Table 1. As seen, the framework Al/P ratio is usually below unity, which is clearly a result of some PO bonds being occupied by molecules of template. Moreover, the composition of the inorganic layers remains relatively constant even when there is an excess of aluminum in the synthesis gel.

From Figure 3, it is apparent that $AlPO_4$ 1:0.8:1:60 (sample no. 4), which showed an XRD pattern with very intense and sharp peaks (Figure 1), has only small amounts of extraframework aluminum. When the alumina concentration was further decreased (sample nos. 1 and 2), only a sharp ^{27}Al NMR peak at ca. −10 ppm remained, corresponding to the hydrated six-coordinated aluminum in aluminophosphate framework.

^{31}P MAS-NMR spectra of essentially the same series of samples with increasing Al/P ratios (sample nos. 20, 1−6, and 8−10) are shown in Figure 5. The aluminum free sample (sample no. 20) exhibited two overlapped ^{31}P NMR signals at 2.3 and 0.6 ppm with relative intensities of 40 and 60%, respectively. These shifts are common for acid ammonium salts of phosphoric acid. The chemical shift anisotropy parameters, obtained from the simulation of the spinning sidebands patterns at different spinning speeds as well as static spectra, were found to be very similar for both sites. The anisotropy ($\Delta\delta$) and the asymmetry parameter (η) were −75 ± 5, and 0.3 ± 0.1, respectively. On the basis of these parameters and isotropic chemical shifts, these two peaks can be assigned to nonequivalent isolated $PO_2(OH)_2$ groups[38] forming the inorganic layers of the template−phosphoric acid complex. It is inferred that this complex is most likely to be dodecylammonium dihydrogen phosphate.

The reported chemical shifts of ^{31}P in microporous $AlPO_4$-type materials generally fall in the range −19 to −30 ppm.[36,39,40] The shift of the ^{31}P NMR signal to lower fields can be caused by several factors. The nature of the cations in the second coordination sphere of phosphorus appears to be the most significant one.[36] Monovalent cations, acid protons, and coordinated water can all cause downfield chemical shifts in the spectra of phosphates. To a first approximation, the ^{31}P chemical shift of aluminophosphates changes additively with the number of Al in the second coordination shell of phosphorus.[41] It has also been established that the ^{31}P signals are further downfield for the phosphorus species containing highly coordinated aluminum than for those containing only 4-coordinated aluminum.[42] The presence of P−OH groups and ammonium cations should also shift the signals to lower field.

Our $AlPO_4$ samples with an Al/P ratio in the range 0.8−1.6 (sample nos. 4−8) gave similar ^{31}P NMR spectra with a broad signal centered at about −13 ppm. On the basis of literature data, the occurrence of the chemical shift at ca. −13 ppm (Table 2 and Figure 5) may be attributed to tetrahedral phosphorus bonded to (4-X) aluminum tetrahedra and X hydroxyl groups (where X = 1 or 2). As pointed out by Saldarriaga et al.,[43] the chemical shift of ^{31}P in molecular sieves can also be affected by the hydrophilic nature of the materials. Since these lamellar aluminophosphate materials are expected to contain large amounts of water between their layers, a change in the chemical shift of ^{31}P NMR is not surprising. The broadening of the ^{31}P NMR signals in these samples (sample nos. 4−10, Figure 5) stems from the distribution of phosphorus among sites with slightly different environments. The fact that the line shape is dominated by a distribution in the chemical shifts was confirmed by the preservation of the peak shape at higher field (see caption of Figure 5). If the observed broadening was due to several overlapping but distinct signals, an improvement of the signal resolution would have been observed. The first derivative of the ^{31}P NMR signal shows the presence of at least five components (Figure 5, inset); however, the overall broadening of the signals does not allow us to draw definite assignments of the various phosphorus environments. Nevertheless, the range of observed chemical shifts does exclude the occurrence of P sites with P in their second coordination shells.[36,38]

For samples with very low Al contents (sample nos. 1 and 2), whose XRD patterns were similar to that of Al-free surfactant−phosphoric acid complex (sample no. 20, Figure 1), there was a sharp peak at −19 ppm in addition to the ^{31}P peak close to 0 ppm observed in the Al-free sample. The origin of this line is not clear. In the ^{27}Al spectra of the same samples we observe a sharp signal at around −10 ppm. If the ^{27}Al and ^{31}P signals belong to the same compound, it could have a structure very close to that of variscite, $AlPO_4 \cdot 2H_2O$ ($\delta(^{31}P)$ =

(36) Moudrakovski, I. L.; Schmachlova, V. P.; Katsarenko, N. S.; Mastikhin, V. M. *J. Phys. Chem. Solids* **1987**, *47*, 335.
(37) Rocha, J.; Kolodziejski, W.; He, H.; Klinowski, J. *J. Am. Chem. Soc.* **1992**, *114*, 4884.
(38) Hartman, P.; Vogel, J.; Schnabel, B. *J. Magn. Reson.* **1994**, *111*, 110.
(39) Muller, D.; Jahn, E.; Fahlke, B.; Ladwig, G.; Haubenreisser, U. *Zeolites* **1985**, *5*, 53.
(40) Blackwell, C. S.; Patton, R. L. *J. Phys. Chem.* **1984**, *88*, 6135.
(41) Fedotov, M. A.; Moudrakovski, I. L.; Mastikhin, V. M. *Izv. Akad. Nauk SSSR, Ser. Khim.* **1987**, *10*, 2340.
(42) Barrie, P. *Spectroscopy of New Materials*, Wiley: New York, 1993; p 151.
(43) de Saldarriaga, L. S.; Saldarriaga, C.; Davis, M. E. *J. Am. Chem. Soc.* **1987**, *109*, 2686.

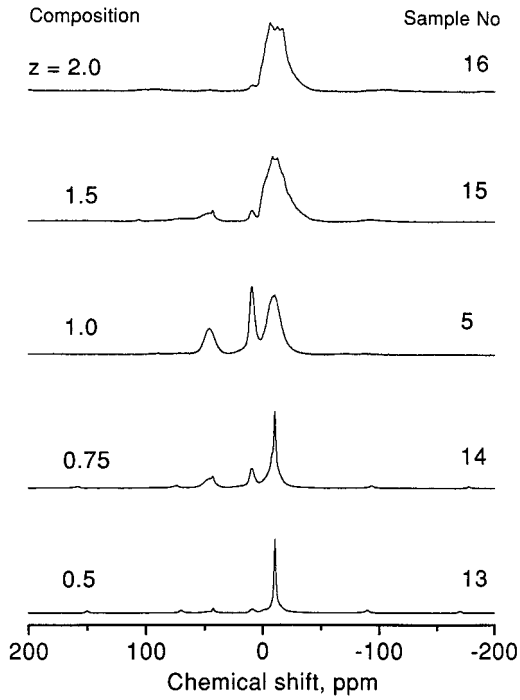

Figure 6. ^{27}Al NMR spectra of $AlPO_4$ 1:1:z:60 samples prepared with variable amounts of template.

−19.5 ppm, $\delta(^{27}Al) = -11.3$ ppm[35,41,44,45]). The small width of the lines for both nuclei indicates a high local ordering. The variscite has a very distinct X-ray pattern, and at the concentration indicated by NMR this phase should be observed by XRD. However, this is true only if we have a long-range ordering. If only small clusters of the compound are randomly distributed throughout the template−phosphoric acid complex, their XRD peaks may be very difficult to detect.

Samples with high levels of Al (sample nos. 9 and 10) display the broad ^{31}P signal centered at ca. −13 ppm discussed earlier, in addition to a low-intensity (less than 4% of total intensity), sharp peak at ca. −3.4 ppm attributed to a separate impurity phase.

Influence of Surfactant/P_2O_5 Ratio. Using the following molar gel composition, P_2O_5:Al_2O_3:z$C_{12}H_{25}NH_2$:60H_2O, a series of samples were prepared with different template/P_2O_5 ratios ($z = 0.125-2.0$). Only the samples prepared with $z = 0.75$ and 1.0 were pure phases with good crystallinity and almost the same d spacing of 32.5 Å. One of these phases, i.e., $AlPO_4$ 1:1:1:60 (sample no. 5) has already been described above. The samples prepared with $C_{12}H_{25}NH_2/P_2O_5$ ratios of 0.125 and 0.25 were amorphous and samples with $z =$ 0.5, 1.5, and 2.0 ratios consisted of mixtures of two phases with d spacings of 36.5 and 32.5, 37.1 and 30.7, and 37.7 and 30.3 Å, respectively (Table 1). These phases were different from the material obtained with $z = 0.75$ and 1.0 ratios ($d_{001} = 32.5$ Å). The presence of different phases in these samples is reflected in their ^{31}P and ^{27}Al NMR spectra.

^{27}Al NMR spectra of samples with $C_{12}H_{25}NH_2/P_2O_5$ ratios of 0.5−2.0 are shown in Figure 6. At ratios below 1.0, a sharp signal was observed at ca. −10 ppm which we previously have tentatively attributed to clusters of hydrated aluminum orthophosphate dispersed in the layers of the template−phosphoric acid complex. For the ratio of 0.5 this was the only signal observed. At the ratio of 0.75 the additional lines with positions observed for lamellar aluminophosphate phase were present. The total intensity of these lines was more than twice that of the sharp signal at −10 ppm. The spectra of the samples prepared with the highest concentrations of template show a new broad signal with a line shape characteristic of second-order quadrupolar interaction. For the sample with $C_{12}H_{25}NH_2/P_2O_5 = 1.5$, two structureless signals centered at ca. 10 and 45 ppm, as previously observed for most samples, were also present.

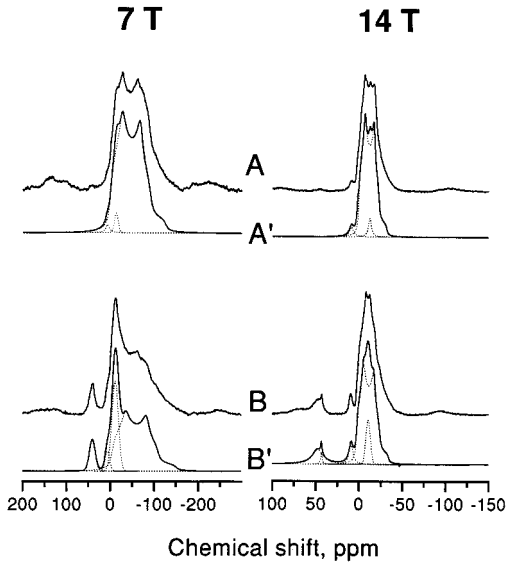

Figure 7. ^{27}Al NMR spectra of $AlPO_4$ 1:1:z:60 samples with $z = 2$ (sample no. 16) and $z = 1.5$ (sample no. 15; spectra A and B, respectively) recorded at two different fields and their simulations (A′ and B′).

The experiments at different magnetic fields show that the major contribution to the spectrum of the sample with $C_{12}H_{25}NH_2/P_2O_5 = 1.5$ and 2.0 is made by the same signal with quadrupolar splitting. Both spectra have a noticeable residual structureless signal at around −11 ppm, which could be a result of distortions/defects of the main phase. Note that multifield measurements help separate the residual part of the signal from the main signal quite accurately (see Figure 7). The parameters of the quadrupolar interaction and the isotropic chemical shift determined from the simulation of the spectra recorded at different magnetic fields were as follows: isotropic chemical shift of the species $\delta_i = 3$ ppm, quadrupolar interaction constant $C_q = 7.5$ MHz ($C_q = e^2qQ/h$), asymmetry parameter $\eta = 0.35$. Such a large quadrupolar constant indicates a very low symmetric aluminum oxygen environment and to our knowledge has been observed in aluminophosphates only once in $AlPO_4$-21 for pentacoordinated aluminum.[45]

Since this line is responsible for a major part of the signal, it can be attributed to the aluminum in the dominant phase with $d = 37.7$ Å. The other phase detected by XRD is probably formed solely by template−phosphoric acid interaction. Detailed assignment of the observed line is far from trivial. While the chemical shifts in the region of 2−10 ppm are normally attributed to six-coordinated aluminum, pentacoordinated alumi-

(44) Mastikhin, V. M.; Lapina, O. B.; Moudrakovski, I. L. *Application of Nuclear Magnetic Resonance in Heterogeneous Catalysis*; Nauka-Press: Novosibirsk, 1992; p 1.

(45) (a) Jelinek, R.; Chmelka, B. F.; Wu, Y.; Grandinetti, P. J.; Pines, A.; Barrie, P. J. *J. Am. Chem. Soc.* **1991**, *113*, 4097. (b) Freude, D.; Haase, J. In: *NMR Basic Principles and Progress*; Springer-Verlag: Berlin, 1993; Vol. 29, p 1.

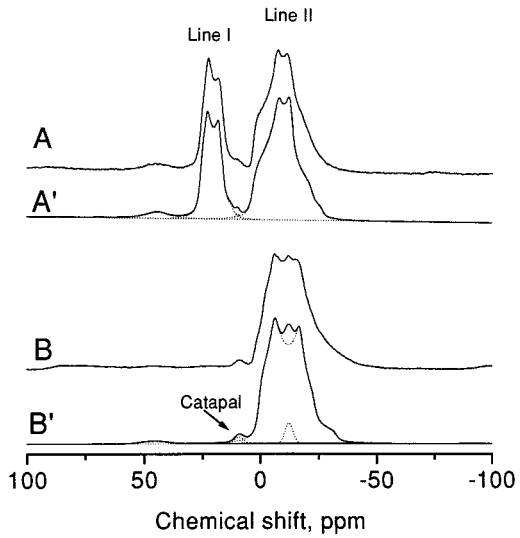

Figure 8. ^{27}Al NMR spectra of $AlPO_4$ 1:1:2:60 (sample no. 16) after vacuum treatment for 140 h (A) and after rehydration in water vapor (B). A′ and B′ are corresponding simulations.

num could contribute at this region as well. For example, Rocha et al.[37] in one case reported a chemical shift of 6.5 ppm for pentacoordinated aluminum. While the five-coordinated state for aluminum in aluminophosphates is not so uncommon as in aluminosilicates, we would not attribute the observed line to this state based only on these parameters. Additional information about the actual state of aluminum in this material was obtained from NMR measurements of vacuum-treated samples. After being kept in vacuum for 140 h, $AlPO_4$ 1:1:2:60 (sample no. 16) produced a complex ^{27}Al spectrum consisting of two lines with quadrupolar splitting. These signals can be unambiguously resolved only at the highest available magnetic field (Figure 8A). The parameters of these signals were as follows: Line I: $\delta_i = 26.9$ ppm, $C_q = 4.9$ MHz, $\eta = 0.3$. Line II: $\delta_i = 4.0$ ppm, $C_q = 6.8$ MHz, $\eta = 0.65$. All parameters of line I unambiguously point to five-coordinated aluminum.[45] The assignment of line II is not so obvious. While the chemical shift falls well into the region of six-coordinated aluminum, no such large C_q and η have been reported before for AlO_6 sites in aluminophosphates. The values, however, are not abnormal for AlO_6 in aluminum salts,[45b] aluminoborates,[46] or aluminosilicates.[47] Considering all these facts, we assign line II to AlO_6 species with a very asymmetric oxygen environment.

Exposure of the evacuated samples to water vapor completely restores their spectra to that of untreated samples (Figure 8B, compare to the right-hand side of Figure 7A). This fact shows that the removal of water is the only factor responsible for all the changes observed upon evacuation. The process is completely reversible, which may mean that the desorption of coordinated water does not produce any dramatic changes in the aluminophosphate framework. It is worth noting that the NMR parameters for AlO_6 sites in vacuum-treated samples are significantly different from those in hydrated ones, which is likely a result of the influence on the chemical shift of the second coordination shell

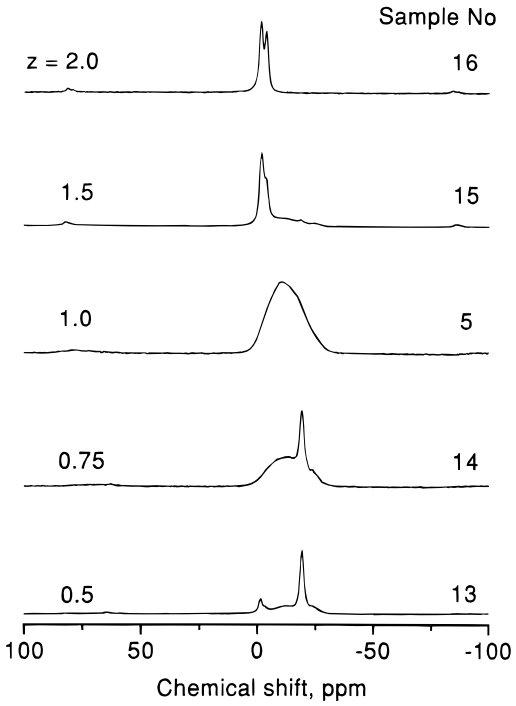

Figure 9. ^{31}P NMR spectra of $AlPO_4$ 1:1:*z*:60 samples prepared with variable amounts of template.

composition. We have also found that the vacuum treatment produces only very small concentration of tetrahedrally coordinated species (Figure 8A). Pentacoordinated aluminum seems to be the preferred species.

Figure 9 shows the ^{31}P NMR spectra of a series of $AlPO_4$ samples prepared with different amounts of template. At a template to P ratio of 0.5 the most intense ^{31}P NMR signal was observed at about −19 ppm, assigned earlier to PO_4 tetrahedra in clusters of aluminum orthophosphate dispersed in the template−phosphoric acid complex. This signal sits on top of the broad line centered at about −13 ppm discussed earlier. (Much smaller peaks were also observed near −1 to −4 ppm). As the ratio of template to P increased ($z = 0.75$ and 1) the broad signal developed and the peak at −19 ppm disappeared. However, when the ratio reached 1.5, two sharp signals appeared at −1.4 and −3.7 ppm. At the highest concentration of template the broad line disappeared completely, and only the sharp signals persisted. The narrowness of these lines indicates a high level of local ordering in the system. Two close, but nevertheless distinct environments for phosphorus are present in the structure of the inorganic layers. The downfield chemical shifts of these lines relative to those observed in microporous aluminophosphates[41] may indicate that each phosphorus tetrahedron in the lattice is linked to two molecules of the protonated template.

We have also prepared a sample using high concentrations of both Al and template (P_2O_5:$2Al_2O_3$:$2C_{12}H_{25}NH_2$:$60H_2O$). This sample showed only one sharp ^{31}P NMR signal at −3 ppm (Figure 10A). The ^{27}Al NMR spectrum consisted of two signals of roughly equal intensities (Figure 10B). As before, the signal at ca. 10 ppm was assigned to extra framework octahedral Al species. The other ^{27}Al NMR signal corresponds to a six-coordinated aluminum species with strong quadrupolar interaction. The parameters of this line are as follows: isotropic chemical shift $\delta_i = 2.3$ ppm, quadrupolar coupling constant $C_q = 7.3$ MHz, and asymmetry

(46) Kunath, G.; Losso, P.; Steuernagel, S.; Schneider, H.; Jager, C. *Solid State Nucl. Magn. Reson.* **1992**, *1*, 267.
(47) Lipmaa, E.; Samoson, A.; Magi, M. *J. Am. Chem. Soc.* **1986**, *108*, 1730.

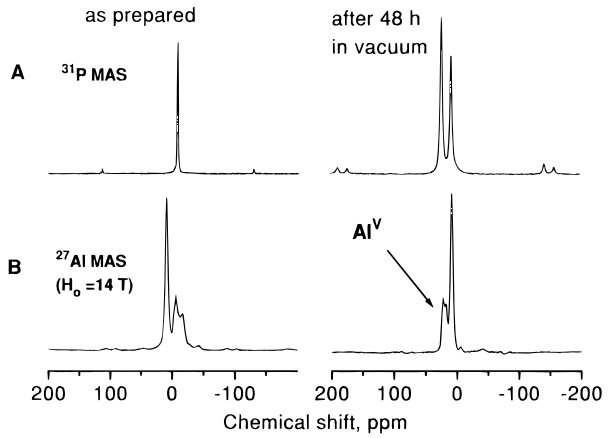

Figure 10. ^{31}P and ^{27}Al NMR spectra of $AlPO_4$ 1:2:2:60 before and after evacuation at room temperature for 48 h.

parameter $\eta = 0.3$. It is important to note that after 48 h evacuation at room temperature most of the framework Al is transformed into a pentacoordinated species showing a new signal with distinct quadrupolar splitting (Figure 10B). The observed chemical shift $\delta_i = 27.4$ ppm and parameters of quadrupolar interaction $C_q = 5.1$ MHz and $\eta = 0.35$ are quite common for pentacoordinated Al in aluminophosphate systems.[42] The almost quantitative transformation of six-coordinated framework Al to pentacoordinated species is consistent with the presence of not more than two sheets of mixed oxides in the aluminophosphate layer. In this case, both sides of the inorganic layer are easily accessible from the interlayer space, and the water coordinated to aluminum could be easily removed. The more deeply located water could hardly be removed under such mild conditions.

Influence of the Amine Chain Length. Five samples were prepared using the gel composition P_2O_5:Al_2O_3:$C_nH_{2n+1}NH_2$:$60H_2O$ with $n = 8$, 10, 12, 14, and 16. For $n = 8$, 10, and 12, only one lamellar phase with $d_{001} = 28.0$, 30.1, and 32.5 Å, respectively, was formed. $C_{14}H_{29}NH_2$ gave a mixture of two layered phases with d spacings of 36.8 and 41.3 Å. Similarly, two layered phases with d spacings of 37.1 and 41.7 Å were obtained in the presence of hexadecylamine. However, everything else being equal, using half of the amount of tetradecyl- and hexadecylamine afforded pure $AlPO_4$ phases with intermediate d spacings of 38.7 and 39.7 Å, respectively.

Influence of H_2O/P_2O_5 Ratio. Using the following molar gel composition (P_2O_5:Al_2O_3:$C_{12}H_{25}NH_2$:wH_2O), a series of $AlPO_4$ samples with H_2O/P_2O_5 ratios of 60, 100, 150, 200, and 300 were prepared. The same lamellar phase with d spacing of 32 Å was formed up to w = 150. However, at H_2O/P_2O_5 ratios of 200 and 300, an additional $AlPO_4$ phase developed. This phase had a higher d spacing ($d_{001} = 36.2$ Å) and corresponded to about 50% of the sample with $w = 300$. Crystallization of the $AlPO_4$ 1:1:1:300 at 373 K for 4 days instead of 1 day led to a single lamellar phase with d spacing of 37.0 Å.

Primary vs Tertiary Amines as Templates. A series of samples were prepared using the gel composition P_2O_5:Al_2O_3:$C_{12}H_{25}N(CH_3)_2$:$60H_2O$, with $y = 1.0$–1.8. The highest crystallinity was obtained at Al/P ratio (in the gel) of 1.2. The d spacing was 26.3 ± 0.3 Å regardless of the overall Al content of the synthesis mixture.

In the case of primary amines, $AlPO_4$ could be prepared even at room temperature within 5 min. However, in the presence of tertiary amines, higher temperatures were necessary for the crystallization to take place. Under otherwise identical conditions, the d spacing of materials obtained with primary amines were always higher than those obtained in the presence of the corresponding tertiary alkyldimethylamines. For example, gels with the composition P_2O_5:Al_2O_3:R–$N(CH_3)_2$:$60H_2O$ gave lamellar phases with $d_{001} = 18.2$ and 26.3 Å, respectively, compared to 28.0 and 32.5 Å in the presence of the corresponding primary amines. This is consistent with earlier observations concerning mesoporous silicate molecular sieves. The so-called HMS, hexagonal mesoporous silicates, prepared in the presence of primary amines had higher d_{100} spacings than the MCM-41 silicates prepared with the corresponding quaternary alkyltrimethylammonium surfactant.[2a] But both materials had similar average pore sizes. The higher d spacing of HMS materials was attributed to their thicker walls as compared to MCM-41. In the case of ionic surfactants, it was argued that this thickness is determined by the electrostatic repulsion between the negatively charged surfaces of the wall regardless of the chain length of the surfactant.[12] In the presence of a *neutral* surfactant such as amines, the wall may grow thicker because of the absence of electrostatic limitations. In our case however, even though amines were used, they were actually protonated. It is therefore likely that the mechanism based on charge matching applies.[3,12] The difference between the d spacing of lamellar $AlPO_4$'s prepared in the presence of primary and tertiary amines is most likely due to different thicknesses of the organic double layer rather than the thickness of the inorganic wall. This may be due to a higher degree of interpenetration of the hydrophobic tails in the case of tertiary amines than the corresponding primary amines. The lower charge density of the hydrophobic heads of protonated tertiary amines compared to that of protonated primary amines allows for thinner organic bilayers.

^{27}Al and ^{31}P NMR spectra of the samples prepared with tertiary amines reveals no significant differences from the spectra of the samples synthesized with primary amines.

Conclusions

We have demonstrated that a variety of aluminophosphate materials with lamellar structures could be synthesized using long-chain primary and tertiary alkylamines as templates. The so-called liquid-crystal templating mechanism was extended for the first time to aluminophosphates. NMR studies have provided strong evidence that these materials have $AlPO_4$ type frameworks and reveal the coordination state of phosphorus and aluminum in the structure of the materials. These lamellar aluminophosphates are thermally unstable when calcined, and the organic moiety could not be removed by solvent extraction. The synthesis variables, namely, (i) the Al/P ratio, (ii) the surfactant/P ratio, (iii) the H_2O/P ratio, (iv) the nature of the template, (v) the crystallization temperature, and (vi) the crystallization time have considerable influence on the quality of the product formed and on the connectivities of Al and P. As in the case of most other oxides studied so far, the

phase diagram of phosphate or aluminophosphate species in the presence of water and long-chain amines is dominated by lamellar phases.

Acknowledgment. Partial funding by the Natural Sciences and Engineering Research Council (NSERC) of Canada is acknowledged. J.S.R. thanks NSERC for awarding the Canada International Fellowship. We are grateful to V. R. Karra for the preparation of some samples. Since the submission of this paper, Oliver et al.[48] published a series of papers dealing with the surface structure of lamellar aluminophosphates prepared in the presence of decylamine in tetraethylene glycol.

CM960029V

(48) (a) Oliver, S.; Kuperman, A.; Coombs, N.; Lough, A.; Ozin, G. A. *Nature* **1995**, *378*, 47. (b) Ozin, G. A.; Oliver, S. *Adv. Mater.* **1995**, *7*, 943. (c) Oliver, S.; Coombs, N.; Ozin, G. A. *Adv. Mater.* **1995**, *7*, 931.